NANO LETTERS

Letter

pubs.acs.org/NanoLett

Selective Control of Gliding Microtubule Populations

Till Korten,[†,∥] Wolfgang Birnbaum,[‡,∥] Dirk Kuckling,[*,‡] and Stefan Diez[*,§,†]

[†]Max Planck Institute of Molecular Cell Biology and Genetics Dresden, Dresden, Germany

[‡]Department of Chemistry, University of Paderborn, Paderborn, Germany

[§]B CUBE, Center for Molecular Bioengineering, Technische Universität Dresden, Dresden, Germany

Supporting Information

ABSTRACT: First lab-on-chip devices based on active transport by biomolecular motors have been demonstrated for basic detection and sorting applications. However, to fully employ the advantages of such hybrid nanotechnology, versatile spatial and temporal control mechanisms are required. Using a thermo-responsive polymer, we demonstrate the selective starting and stopping of modified microtubules gliding on a kinesin-1-coated surface. This approach allows the self-organized separation of multiple microtubule populations and their respective cargoes.

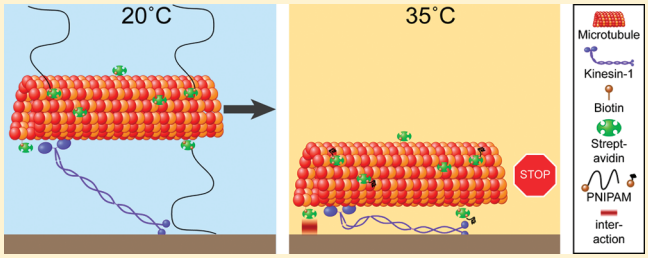

KEYWORDS: *Bionanotechnology, microtubules, kinesin, differential control, molecular sorting*

Motor-driven microtubules have been successfully applied as molecular shuttles in basic nanotechnological transport, detection, and sorting devices.[1−20] However, the lack of precise and flexible spatiotemporal control mechanisms has seriously hampered their application in more complex lab-on-chip systems. The sorting schemes demonstrated so far either sort microtubules globally by length[5,20] or on an individual basis by active steering.[3,9] Unfortunately, both approaches have severe limitations when cargo transported by the microtubules is to be sorted. Sorting by length is only useful if cargo is specifically attached to microtubules of a given length. This requires the microtubules to be first sorted by length, then to be fuctionalized to bind the desired cargo, and eventually to be sorted again after actual cargo binding. Apart from being complex, this approach is additionally hampered by the fact that even stabilized microtubules change their length by breaking, growing, and shrinking.[21,22] On the other hand, steering individual microtubules is tedious, requires complex hardware for detection and control, and severely limits throughput. In contrast, nature has a much more elegant approach to organize microtubule-based transport: In neurons, the microtubules of the axon and of the dendrites are characterized by different post-translational modifications. These modifications cause different types of motors to preferentially move in axons or dendrites, respectively.[23−26] In an analogous approach, we have developed a methodology where different microtubule populations are generated by chemical modification. When gliding on a kinesin-1-coated surface, these populations can be differentially controlled by an external signal. Consequently, a particular microtubule population, and any cargo attached to it, can be separated from the other microtubule transporters. We thereby demonstrate a novel technique that enables enhanced temporal control over motor-based microtubule transport systems and may provide an effective means of automated molecular sorting.

To gain external control, microtubules were functionalized with the thermo-responsive polymer poly(*N*-isopropylacrylamide) (PNIPAM) that has a lower critical solution temperature (LCST) of about 32−33 °C.[27] The polymer chains are dehydrated and form compact structures in water when the solution temperature is above their LCST but become extended structures by hydration when cooled down below the LCST (Figure 1). For our experiments we developed a method to modify one end of each PNIPAM chain with exactly one biotin molecule. Thus, the strong biotin−streptavidin bond could be used to directionally link biotinylated PNIPAM chains to microtubules.

Synthesis of Biotinylated PNIPAM. Biotinylated PNIPAM was synthesized using a biotin-containing initiator, for which the following new synthesis route was developed (Figure 2). In a first step, the primary amine group of 2-(2-aminoethoxy)ethanol was protected by addition of anhydrous HCl (1.01 M 2-(2-aminoethoxy)ethanol and 1.14 M HCl in anhydrous 1,4-dioxane). The solvent was removed under reduced pressure, and the residue dried in vacuum. Subsequently, the product was charged under argon, and the hydroxyl group was reacted at 0 °C with 2-chloropropanoyl chloride (0.22 M 2-(2-aminoethoxy)ethanol hydrochloride and 0.23 M 2-chloropropanoyl chloride in anhydrous acetonitrile). After stirring the reaction mixture at room temperature overnight, the solvent was removed under reduced pressure, and the precipitate was washed with diethyl ether and dried in vacuum to yield the

Received: October 14, 2011
Revised: November 17, 2011
Published: December 12, 2011

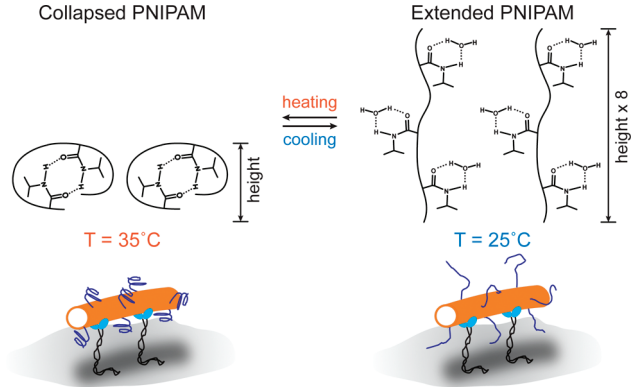

Figure 1. Thermo-responsive PNIPAM polymers directionally linked to microtubules. PNIPAM switches between a collapsed state at temperatures above its LCST (left) and an extended state at temperatures below its LCST (right). When attached to microtubules gliding on a kinesin-1-coated surface, these polymers can switch the motility behavior.

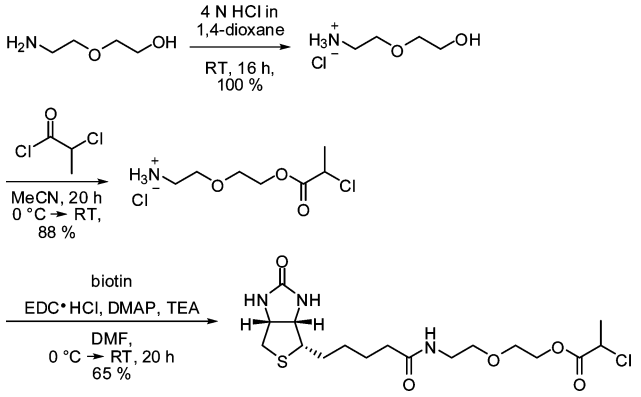

Figure 2. Synthesis of the biotinylated initiator. The free amino group is protected through hydrochloride in the first step. Subsequently only the hydroxyl group reacts with the 2-chloropropanoyl chloride to give the intermediate amino-terminated initiator. The biotinylated initiator is formed by coupling the amino-terminated initiator with biotin.

amino-terminated initiator. In the last step, a *N*,*N*-dimethylformamide solution of 0.22 M amino-terminated initiator, 0.21 M D(+)-biotin and 0.03 M 4-(dimethylamino)pyridine was prepared and charged under argon. The primary amine group of the initiator was deprotected by the addition of 0.22 M triethylamine and by stirring the solution for 20 min at room temperature. Then, 0.22 M *N*-(3-dimethylaminopropyl)-*N*′-ethylcarbodiimide hydrochloride was added at 0 °C to couple the D(+)-biotin to the free amine group of the initiator. The reaction mixture was stirred overnight at room temperature, and the solvent was removed by distillation afterward. The received crude product was purified by treatment with cold water, and the precipitate was collected and dried in vacuum to finally obtain the biotinylated initiator. The major advantage of this approach is that the intermediate product before addition of the biotin residue is an amino-terminated initiator. This amino-terminated initiator can be stored and used for other purposes, such as direct covalent coupling to biomolecules, fluorescent labeling, or surface attachment, gaining a highly flexible tool for PNIPAM functionalization and making the synthesis described here more versatile than a previous approach.[28] From the biotin initiator, PNIPAM was then synthesized by atom transfer radical polymerization (ATRP).[29] The average molecular weight was 40 kDa with a dispersity of 1.2 (determined by size exclusion chromatography, using PMMA standards for calibration and *N*,*N*-dimethylacetamide as solvent). Comparison with previous atomic force spectroscopy measurements[30] suggests that this molecular weight corresponds to a contour length of approximately 70 nm for the fully stretched polymer chains. On the other hand, the chains in solution will have a much smaller radius of gyration. For a 10 MDa molecule, the radius of gyration was measured to be ≈130−160 nm in the extended state of PNIPAM and ≈20 nm in the collapsed state.[31,32] Assuming the PNIPAM used here has the same relative volume, we estimate the radii of gyration of the extended and collapsed chains to be ≈20 and ≈3 nm, respectively.

Preparation of PNIPAM-Coated Microtubules. Biotinylated PNIPAM was linked to microtubules via streptavidin. Therefore, biotinylated microtubules were polymerized from a mixture of rhodamine-labeled, biotinylated, and unlabeled tubulin (unless specified otherwise, a ratio of 3:4:9 rhodamine-labeled:biotinylated:unlabeled tubulin was used) in polymerization buffer (32 μM total tubulin, 5% DMSO, 5 mM $MgCl_2$, 1 mM EDTA, 80 mM PIPES/KOH, and pH of 6.9). This microtubule population was mixed with a population of control microtubules (nonbiotinylated, a ratio of 1:4 fluorescein-labeled:unlabeled tubulin). The microtubule mixture was injected into flow channels coated with kinesin-1 motor molecules (prepared as described in note 33). Unbound microtubules were washed out with 15 μL of motility solution. Afterward, the microtubules were coated with streptavidin using 15 μL of 0.5 mg/mL streptavidin in motility solution. Streptavidin coating of the microtubules was assessed by comparing the speeds of biotinylated and nonbiotinylated microtubules. Biotinylated, rhodamine-labeled microtubules were ≈40% slower than nonbiotinylated, fluoresceine-labeled microtubules, indicating successful selective streptavidin coating of biotinylated microtubules. Compared to previously published results obtained under similar conditions,[14] this corresponds to a streptavidin coating of approximately every sixth tubulin dimer (16%). After streptavidin coating, microtubule gliding was stopped with a motility solution where ATP was substituted by 250 μM adenosine 5′-[β,γ-imido] triphosphate (AMPPNP). From then on the temperature was controlled using a self-constructed temperature stage which allows rapid heating and cooling using a peltier element.[34,35] With the temperature set to 20 °C (to improve solubility of the PNIPAM), the assay was incubated for 30 min with a solution of 333 μM biotinylated PNIPAM in BRB80 supplemented with 250 μM AMPPNP, 10 μM taxol, and 10 mM DTT. Unbound PNIPAM was washed out with AMPPNP motility solution.

Temperature Control of PNIPAM-Coated Microtubules. After PNIPAM coating of microtubules, the chamber was heated to 35 °C. Microtubule gliding was restarted by perfusion with ATP-containing motility solution. Subsequently, microtubule gliding was imaged by dual-color, time-lapse fluorescence microscopy; alternating images in the fluorescein and the rhodamine channel were acquired, each with a rate of 1 image every 4 s. During recording, the temperature was switched repeatedly between 35 and 20 °C, approximately every 2 min (Figure 3A and movie 1, Supporting Information). At temperatures above the LCST (35 °C, collapsed state of PNIPAM), almost all PNIPAM-coated microtubules (shown in red in Figure 3) were stuck to the surface (18 out of 19 microtubules). Upon switching to temperatures below the

dx.doi.org/10.1021/nl203632y | *Nano Lett.* 2012, 12, 348−353

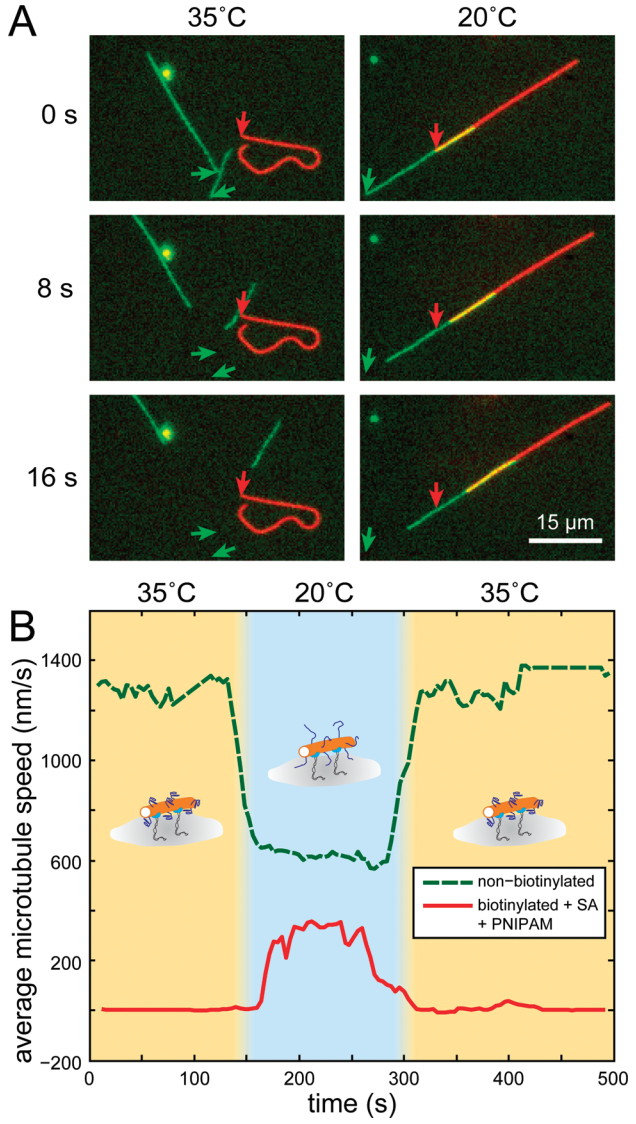

Figure 3. Reversible starting and stopping of PNIPAM-coated microtubules. Gliding biotinylated microtubules coated with streptavidin and biotinylated PNIPAM (red) and nonbiotinylated control microtubules (green) were taken through a cycle of switching from 35 to 20 °C and back. (A) Typical fluorescence images of gliding microtubules over a timespan of 16 s. The positions of the microtubule's trailing ends in the first frame are indicated by arrows in the respective color. (B) Median of the gliding speeds of 1−6 nonbiotinylated microtubules and 8−13 streptavidin and PNIPAM-coated microtubules as function of time. The speeds of individual microtubules were calculated as follows: The walked distance between each frame was measured as a function of time.[36] The speeds in each frame were then determined by a gliding average over 5 (20 s window; nonbiotinylated) or 7 (28 s window; biotinylated + SA + PNIPAM) frames.

LCST (20 °C, extended state of PNIPAM), the majority of the PNIPAM-coated microtubules started to glide (10 out of 18 microtubules). Some microtubules remained partially stuck to the surface (4 out of 18 microtubules) or were released into solution (4 out of 18 microtubules). In contrast, all 24 nonbiotinylated microtubules observed throughout the experiment (shown in green in Figure 3) kept gliding with speeds depending on the temperature, as expected for an enzyme driven reaction. The successful starting and stopping of the majority of PNIPAM-coated microtubules is also reflected in the average microtubule speeds shown in Figure 3B. Microtubule gliding speeds were evaluated quantitatively using an automated tracking software.[36]

Mechanism of Switching. To understand the mechanism behind the switching, biotinylated and rhodamine-labeled microtubules were coated with PNIPAM in a flow chamber as described above. Then, biotinylated, fluorescein-labeled microtubules were coated with streptavidin outside the flow chamber by incubating them for 5 min with 0.5 mg/mL streptavidin (in BRB80 supplemented with 10 μM taxol). Excess streptavidin was removed by centrifugation in a Beckman air fuge at 27 psi for 5 min and subsequent resuspension of the pellet in motility solution. These streptavidin-coated microtubules were added to the flow chamber after PNIPAM was washed out with AMPPNP motility solution. Thus, two microtubule populations were present in the flow chamber: one that was coated both with streptavidin and PNIPAM and one that was coated with streptavidin alone. Time−distance plots of typical example microtubules, taken through a cycle of temperature switching, are shown in Figure 4A. In addition, the time−distance plot for a typical example nonbiotinylated microtubule (from a neighboring flow chamber that was treated the same as the first flow chamber) is also shown for comparison. Again, the nonbiotinylated microtubule glided smoothly both at 35 and 20 °C (Figure 4 green dashed line). The microtubule coated with both streptavidin and PNIPAM was stuck at 35 °C and was gliding with reduced speed at 20 °C (Figure 4 red solid line). In contrast, the microtubule that was coated with streptavidin alone moved neither at high nor at low temperatures (Figure 4 blue dotted line). The same was true for streptavidin-coated microtubules that were subjected to the procedure described above, including stopping motility with AMPPNP and heating to 35 °C, except that PNIPAM was omitted completely. This suggests that in our switching scheme, streptavidin plays a crucial role in the stopping of microtubules. In order to analyze the respective effects of streptavidin- and PNIPAM-coating density, we analyzed the switching behavior of microtubule populations with varied biotinylation ratios and PNIPAM incubation times. Figure 4B shows the overall switching quality indices (see eq 1 in note 37) of these populations. With respect to the biotinylation ratio, a ratio of 0.25 (25% biotinylated tubulin used during polymerization) seems to be optimal for motility switching. Lower biotinylation ratios resulted in lower switching qualities, because a large portion of microtubules did not stop at 35 °C. On the other hand, higher biotinylation ratios also decreased the switching quality, because a large portion of microtubules remained stuck even at 20 °C (see also movie 2 top row, Supporting Information). In a similar fashion, an optimal incubation time with PNIPAM (15−30 min) existed for microtubules with a biotinylation ratio of 0.25. Shorter incubation times generated microtubules decorated with a lower PNIPAM density, not sufficient to overcome the streptavidin−surface interaction. Following the same argument, longer incubation times prevented efficient stopping (see also movie 2 bottom row, Supporting Information). These results indicate that a certain amount of streptavidin on the microtubule lattice is necessary to stop gliding. A certain ratio of PNIPAM to streptavidin is then necessary to facilitate successful starting and stopping of the motility.

From our results, we propose the following switching mechanism (Figure 5): After motility was stopped with AMPPNP and the assay was heated to 35 °C, microtubules

dx.doi.org/10.1021/nl203632y | Nano Lett. 2012, 12, 348−353

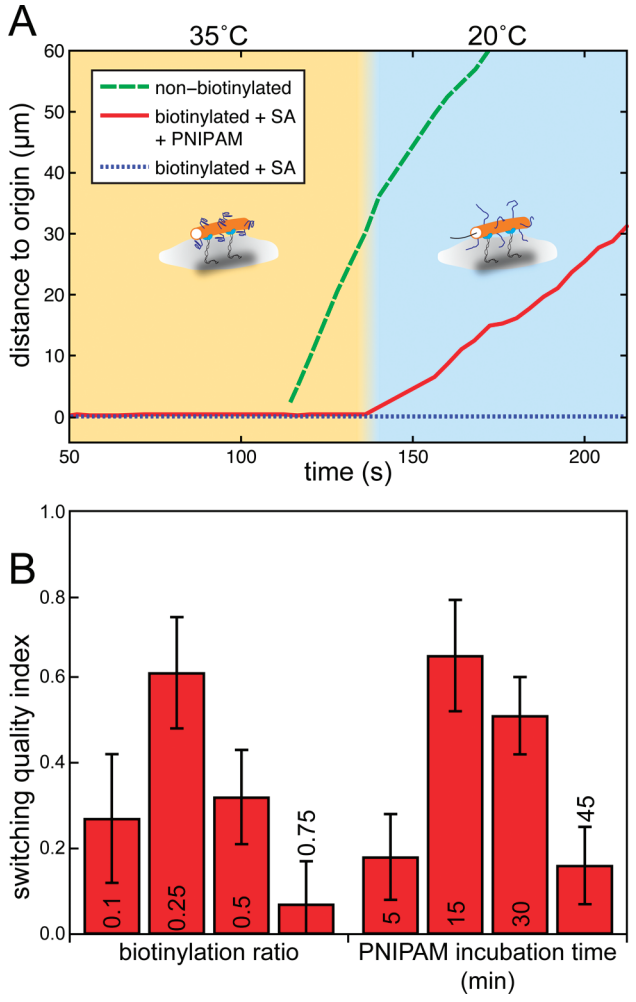

Figure 4. Influence of microtubule biotinylation and PNIPAM density on the switching behavior. (A) Time–distance plots of typical microtubules from populations that were either nonbiotinylated (and thus coated with neither streptavidin nor PNIPAM), biotinylated and coated with streptavidin and biotinylated PNIPAM, or biotinylated and coated with streptavidin only. Each population was observed while switching between 35 to 20 °C (orange and blue backgrounds, respectively) using fluorescence microscopy. Microtubule positions were tracked using the FIESTA software developed in our lab.[36] Insets show drawings of microtubules, decorated with collapsed (35 °C) or extended (20 °C) PNIPAM, gliding on a kinesin-1-coated surface. (B) Switching quality depending on the biotinylation ratio (left; incubation time: 30 min) or the PNIPAM incubation time (right; biotinylation ratio: 0.25). The switching quality index was determined according to eq (1) in note 37.

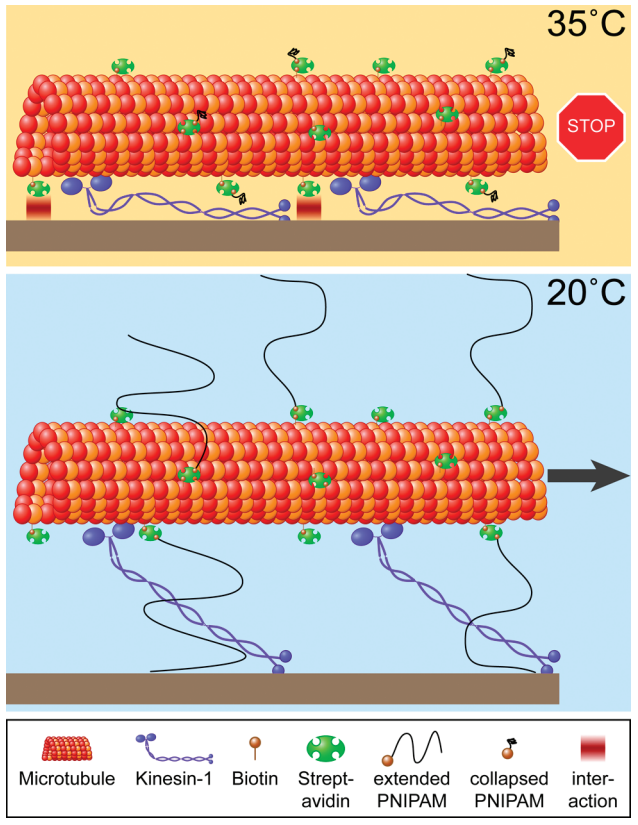

Figure 5. Proposed switching mechanism. Streptavidin-coated microtubules stop at 35 °C when PNIPAM chains are collapsed. This effect occurs also in the absence of PNIPAM and is likely caused by an interaction of streptavidin on the microtubule with the surface. At 20 °C, PNIPAM extends and weakens the streptavidin–surface interaction enough to start gliding motility.

coated with streptavidin alone were permanently stalled. Therefore, we hypothesize that the stopping of streptavidin- and PNIPAM-coated microtubules originates from a streptavidin–surface interaction. There are several likely interaction partners on the surface that could bind to the microtubule-attached streptavidin: (i) The slightly hydrophobic surface itself could interact with the hydrophobic binding pocket of streptavidin, as has been shown for hydrophobic peptides.[38,39] Like all hydrophobic interactions,[40] this interaction will be enhanced at the elevated temperature of 35 °C. (ii) When incubating microtubules with streptavidin, part of this streptavidin likely also binds nonspecifically to the surface. It has been shown that streptavidin has a tendency to aggregate,[41] and thus an interaction between surface- and microtubule-bound streptavidin is plausible. Again, this interaction is expected to be enhanced at 35 °C. (iii) Surface-bound streptavidin could interact with free biotin on the microtubule lattice. However, this is unlikely because we use saturating streptavidin concentrations and do not observe bundling of gliding microtubules, which has been reported for microtubules incubated with nonsaturating streptavidin concentrations.[6] (iv) Biotin–PNIPAM on the microtubules could interact with biotin–PNIPAM on the surface in the collapsed state. While not crucial to the initial stopping of microtubules, this interaction could help in stopping microtubules during a switch from 20 to 35 °C. Independent from which interaction mechanism is mainly responsible for microtubule stopping, this interaction is apparently weakened by extended PNIPAM chains (at 20 °C) on the microtubules, allowing gliding motility. Similar weakening of molecular interactions by PNIPAM has been observed for cell adhesion to surfaces and even for the interaction of PNIPAM conjugated streptavidin with biotin.[42–44] Whether microtubules are released completely into solution or continue to glide possibly depends on the length of the PNIPAM chains. In fact, a release into solution may also offer interesting opportunities: Using hydrodynamic flow released mirotubules could be separated from microtubules that remain gliding.

Summary. We have demonstrated the selective control of different microtubule populations on the same surface. PNIPAM- and streptavidin-coated microtubules were stopped at temperatures above the polymers LCST. At the same time,

dx.doi.org/10.1021/nl203632y | Nano Lett. 2012, 12, 348–353

unmodified microtubules remained gliding. We hypothesize that the stopping at 35 °C is facilitated by streptavidin−surface interactions. These interactions are then weakened by extended PNIPAM chains on the microtubule, thus allowing motility at 20 °C. In combination with directed gliding of microtubules across a heated surface, this could be used to separate different cargoes transported by the two microtubule populations. This possibility is especially intriguing since the control affects the whole microtubule population and does not require sophisticated guiding structures and steering of individual microtubules.[3,9] Therefore our method can improve the performance of integrated and miniaturized microtubule devices. Additionally, this method is not limited to bulk control of the whole microtubule population but could be used to stop individual microtubules, if combined with local heating.[45] Therefore, the starting and stopping of microtubules on the surface by an external signal, as we have demonstrated, represents a significant advancement toward the nanotechnological application of microtubule transport systems.

■ ASSOCIATED CONTENT

Ⓢ Supporting Information

Movie 1 (reversible-switching.avi): Reversible switching of PNIPAM-coated microtubules. Fluorescent time-lapse movie of rhodamine-labeled, biotinylated microtubules that were coated with streptavidin and biotin-PNIPAM (red) and fluorescein labeled, nonbiotinylated microtubules (green).

Movie 2 (biotinylation-time.avi): Dependence of switching on biotinylation of microtubules and PNIPAM incubation time. Fluorescent time-lapse movies of rhodamine-labeled, biotinylated microtubules coated with streptavidin and PNIPAM. Top: the biotinylation ratio was varied from 10% biotinylated tubulin (10% biotinylated) to 50% biotinylated (50% biotinylated). Bottom: the time of incubation with PNIPAM was varied from 5 min (5 min PNIPAM) to 45 min (45 min PNIPAM).

This material is available free of charge via the Internet at http://pubs.acs.org.

■ AUTHOR INFORMATION

Corresponding Author

*E-mail: dirk.kuckling@uni-paderborn.de; diez@bcube-dresden.de.

Author Contributions

‖These authors contributed equally.

■ ACKNOWLEDGMENTS

We would like to thank Dr. Leonid Ionov for fruitful discussions throughout the project and experimental help with initial experiments. This work was funded by the Volkswagen Foundation, the European commission (FP7) under the contract MONAD (NMP4-SL-2009-228971) and the Max-Planck-Society.

■ REFERENCES

(1) Hess, H.; Clemmens, J.; Qin, D.; Howard, J.; Vogel, V. *Nano Lett.* **2001**, *1*, 235−239.
(2) Hess, H.; Vogel, V. *J. Biotechnol.* **2001**, *82*, 67−85.
(3) Jia, L. L.; Moorjani, S. G.; Jackson, T. N.; Hancock, W. O. *Biomed. Microdevices* **2004**, *6*, 67−74.
(4) Bohm, K. J.; Beeg, J.; zu Horste, G. M.; Stracke, R.; Unger, E. *IEEE Trans. Adv. Packag.* **2005**, *28*, 571−576.
(5) Ionov, L.; Stamm, M.; Diez, S. *Nano Lett.* **2005**, *5*, 1910−1914.
(6) Hess, H.; Clemmens, J.; Brunner, C.; Doot, R.; Luna, S.; Ernst, K.-H.; Vogel, V. *Nano Lett.* **2005**, *5*, 629−33.
(7) Nitta, T.; Hess, H. *Nano Lett.* **2005**, *5*, 1337−42.
(8) Bachand, G. D.; Rivera, S. B.; Carroll-Portillo, A.; Hess, H.; Bachand, M. *Small* **2006**, *2*, 381−5.
(9) van den Heuvel, M. G. L.; de Graaff, M. P.; Dekker, C. *Science* **2006**, *312*, 910−4.
(10) Nitta, T.; Tanahashi, A.; Hirano, M.; Hess, H. *Lab Chip* **2006**, *6*, 881−5.
(11) Ramachandran, S.; Ernst, K.-H.; Bachand, G. D.; Vogel, V.; Hess, H. *Small* **2006**, *2*, 330−4.
(12) Brunner, C.; Wahnes, C.; Vogel, V. *Lab Chip* **2007**, *7*, 1263−1271.
(13) Doot, R. K.; Hess, H.; Vogel, V. *Soft Matter* **2007**, *3*, 349−356.
(14) Korten, T.; Diez, S. *Lab Chip* **2008**, *8*, 1441−7.
(15) Lin, C. T.; Kao, M. T.; Kurabayashi, K.; Meyhofer, E. *Nano Lett.* **2008**, *8*, 1041−1046.
(16) Agarwal, A.; Katira, P.; Hess, H. *Nano Lett.* **2009**, *9*, 1170−5.
(17) Bachand, G. D.; Hess, H.; Ratna, B.; Satir, P.; Vogel, V. *Lab Chip* **2009**, *9*, 1661−6.
(18) Fischer, T.; Agarwal, A.; Hess, H. *Nat. Nanotechnol.* **2009**, *4*, 162−6.
(19) Kim, B.; Putkaradze, V.; Hikihara, T. *Phys. Rev. Lett.* **2009**, *102*, 215502.
(20) Sugita, S.; Murase, T.; Sakamoto, N.; Ohashi, T.; Sato, M. *Lab Chip* **2010**, *10*, 755.
(21) Boal, A. K.; Tellez, H.; Rivera, S. B.; Miller, N. E.; Bachand, G. D.; Bunker, B. C. *Small* **2006**, *2*, 793−803.
(22) Jeune-Smith, Y.; Hess, H. *Soft Matter* **2010**, *6*, 1778.
(23) Jacobson, C.; Schnapp, B.; Banker, G. A. *Neuron* **2006**, *49*, 797−804.
(24) Reed, N. A.; Cai, D.; Blasius, T. L.; Jih, G. T.; Meyhofer, E.; Gaertig, J.; Verhey, K. J. *Curr. Biol.* **2006**, *16*, 2166−2172.
(25) Cai, D.; McEwen, D. P.; Martens, J. R.; Meyhofer, E.; Verhey, K. J. *PLoS Biol* **2009**, *7*, e1000216.
(26) Konishi, Y.; Setou, M. *Nat Neurosci* **2009**, *12*, 559−567.
(27) Sun, T.; Wang, G.; Feng, L.; Liu, B.; Ma, Y.; Jiang, L.; Zhu, D. *Angew. Chem., Int. Ed.* **2004**, *43*, 357−60.
(28) Bontempo, D.; Li, R. C.; Ly, T.; Brubaker, C. E.; Maynard, H. D. *Chem. Commun.* **2005**, 4702.
(29) Braunecker, W.; Matyjaszewski, K. *Prog. Polym. Sci.* **2007**, *32*, 93−146.
(30) Goodman, D.; Kizhakkedathu, J. N.; Brooks, D. E. *Langmuir* **2004**, *20*, 3297−3303.
(31) Wang, X.; Qiu, X.; Wu, C. *Macromolecules* **1998**, *31*, 2972−2976.
(32) Wu, C.; Zhou, S. *Macromolecules* **1995**, *28*, 5388−5390.
(33) Microtubule gliding motility assay: four 1.5 mm wide channels on one flow cell were constructed from 22 × 22 and 18 × 18 mm^2 glass coverslips (prepared to be slightly hydrophobic as described in note),[46] joined by small strips of parafilm which were melted by brief heating to ∼100 °C. At room temperature (23 °C), the channels were then perfused sequentially with 15 μL each of a solution of 5 mg/mL casein in BRB80 (1 mM $MgCl_2$, 1 mM EDTA, 80 mM PIPES/KOH, and pH of 6.9; incubation time 5 min), a solution of 2.4 μg/mL kinesin (wild-type drosophila kinesin-1 purified as described in ref 47) in BRB80 supplemented with 2 mg/mL casein, 1 mM ATP and 10 mM dithiothreitol (DTT; incubation time 10 min), and the microtubule mixture described in the text (equivalent of 32 nM tubulin) in motility solution (10 μM taxol, 20 mM D-glucose, 55 μg/mL glucose oxidase and 11 μg/mL catalase, and 1 mM ATP in BRB80; incubation time 5 min).
(34) Korten, T. How Kinesin-1 Deals With Roadblocks: Biophysical Description and Nanotechnological Application. Ph.D. thesis, University of Technology Dresden, 2009; http://nbnresolving.de/urn:nbn:de:bsz:14-qucosa-26443.
(35) Nitzsche, B.; Bormuth, V.; Brauer, C.; Howard, J.; Ionov, L.; Kerssemakers, J.; Korten, T.; Leduc, C.; Ruhnow, F.; Diez, S. *Methods Cell Biol.* **2010**, *95*, 247−271.
(36) Ruhnow, F.; Zwicker, D.; Diez, S. *Biophys. J.* **2011**, *100*, 2820−2828.

(37)

$$\begin{aligned}\text{switching quality index} &= ((35_s - 35_m) + (20_m - 20_s) + SW35_{stop} \\ &+ SW20_{start})/(35_s + 35_m + 20_m + 20_s \\ &+ SW20_{start} + SW20_{rel} + SW20_{stuck} \\ &+ SW35_{stop} + SW35_{gliding}) \end{aligned} \quad (1)$$

where 35_s = number of microtubules stuck to the surface at 35 °C; 35_m = number of microtubules moving at 35 °C; 20_s = number of microtubules stuck to the surface at 20 °C; 20_m = number of microtubules moving at 20 °C; $SW35_{stop}$ = number of microtubules stopping upon switching to 35 °C; $SW35_{gliding}$ = number of microtubules that remain gliding upon switching to 35 °C; $SW20_{start}$ = number of microtubules starting upon switching to 20 °C; $SW20_{rel}$ = number of microtubules released into solution upon switching to 20 °C; and $SW20_{start}$ = number of microtubules remain stuck to the surface upon switching to 20 °C.

(38) Weber, P.; Ohlendorf, D.; Wendoloski, J.; Salemme, F. *Science* **1989**, *243*, 85−88.
(39) Schmidt, T. G.; Skerra, A. *Protein Eng.* **1993**, *6*, 109−122.
(40) Kauzmann, W. *Adv. Protein Chem.* **1959**, *14*.
(41) Bayer, E. A.; Ben-Hur, H.; Hiller, Y.; Wilchek, M. *Biochem. J.* **1989**, *259*, 369−376, PMID: 2719654 PMCID: 1138520.
(42) Ding, Z.; Long, C. J.; Hayashi, Y.; Bulmus, E. V.; Hoffman, A. S.; Stayton, P. S. *Bioconjugate Chem.* **1999**, *10*, 395−400.
(43) Okano, T.; Yamada, N.; Sakai, H.; Sakurai, Y. *J. Biomed. Mater. Res.* **1993**, *27*, 1243−1251.
(44) Stayton, P. S.; Shimoboji, T.; Long, C.; Chilkoti, A.; Ghen, G.; Harris, J. M.; Hoffman, A. S. *Nature* **1995**, *378*, 472−474.
(45) Huber, D.; Manginell, R.; Samara, M.; Kim, B.; Bunker, B. *Science* **2003**, *301*, 352.
(46) Preparation of glass coverslips: Coverslips were sonicated for 15 min in 5% mucasol supplemented with 0.006% diphenyldimethoxysilane, washed with deionized water, and sonicated for 10 min in absolute ethanol. Finally the coverslips were rinsed in deionized and in nanopure (>18 MΩ/m) water and blown dry with nitrogen gas.
(47) Coy, D. L.; Wagenbach, M.; Howard, J. *J. Biol. Chem.* **1999**, *274*, 3667−3671.